ORIGINAL ARTICLE

Improvement of Photocatalytic Activity of TiO_2 Coating by the Modified Sol-gel Method

Mayuko AWATA[1], Masahiro OKADA[2], Takayuki NAMBU[3] and Naoyuki MATSUMOTO[4]

[1]Graduate School of Dentistry (Department of Orthodontics), Osaka Dental University, Osaka, Japan
[2]Department of Biomaterials, Graduate School of Medicine, Dentistry and Pharmaceutical Sciences, Okayama University, Okayama, Japan
[3]Department of Bacteriology, [4]Department of Orthodontics, Osaka Dental University, Osaka, Japan

Synopsis
Photocatalytic TiO_2 was coated on a stainless steel (SUS316L) substrate *via* a sol-gel method at a calcination temperature of 600°C. The sol-gel precursor (titanium isopropoxide) solution was modified by adding crystalline (anatase or rutile) TiO_2 particles to control the crystal phase of the TiO_2 coated on the substrate. The effect of the number of TiO_2 coatings was also evaluated. The TiO_2 coating was characterized by scanning electron microscopy, X-ray diffraction, and X-ray photoelectron spectroscopy. The photocatalytic activity was evaluated from the degradation of methylene blue solution on the TiO_2 coating after UV irradiation. The amount of bacteria adhered on the substrate was also evaluated. The TiO_2 coating comprising a binary phase (anatase/rutile weight ratio = 4.9/5.1) showed the highest photocatalytic activity, which improved after increasing the number of coatings. The amount of bacteria adhered on each TiO_2-coated substrate was not significantly different from that on the uncoated substrate.

Key words: *photocatalytic activity; TiO_2; anatase; rutile; sol-gel method*

Introduction

In recent years, the number of patients in each age group who opt for orthodontic treatment to assist with improved oral hygiene and treatment of malocclusions has been increasing [1-3]. In general, the risk of caries formation and periodontal disease increases during an orthodontic treatment [4-8]. Therefore, long-term management is necessary to obtain good treatment results [9, 10]. During long-term management, the mouth cleaning state of the patient is checked during every hospital visit for the orthodontic treatment, and if the cleaning state is bad, the proper toothbrushing method is explained to the patient, and intraoral cleaning is performed by a dentist or a dental hygienist. To assist with long-term management, a bracket material that possesses properties to help prevent the adhesion of dental plaque or to decompose any adhesive products would be greatly beneficial in the prevention of oral diseases during orthodontic treatment.

Titanium dioxide (TiO_2), which shows photocatalytic action [11-15], has practical applications in the field of air and water purification [16, 17], and is also used as a whitening material in the field of dentistry [18-20]. When light is absorbed into a photocatalyst, excited electrons and holes are formed. These can reduce (electrons) or oxidize (holes) the H_2O sur-

rounding the photocatalyst, causing the generation of free radicals such as hydroxyl (OH) radicals [21]. The OH radicals generated by photoirradiation have a strong oxidation power and will destroy organic compounds around the photocatalyst. Photocatalytic TiO_2 is available generally in two crystal phases – anatase and rutile. A binary crystal phase (*i.e*., a mixture of anatase and rutile) is known to improve the photocatalytic activity, compared to single crystal phases alone [22-27]. Coatings of TiO_2 can be produced by vapor deposition (*e.g*., sputter deposition [28], electron beam evaporation [29], filtered arc deposition [30], and wet chemical (*e.g*., sol-gel method [31,32] techniques. Compared to the vapor deposition techniques that have difficulties forming uniform coatings on substrates with complex shapes, the sol-gel method is independent of the substrate shape and has good control of the coating composition, thickness, and topography [31, 32].

In this paper, we describe the development of orthodontic dental brackets incorporated with photocatalytic antibacterial properties with the ultimate goal of improving oral health during orthodontic treatments. This was accomplished by controlling the crystal phase of a TiO_2 layer formed on a stainless steel substrate, which is generally used as a bracket material [33]. The crystal phase composition was controlled by adding as-prepared rutile TiO_2 particles in a sol-gel method. Furthermore, we compared the photocatalytic activity of samples prepared with different numbers of coatings.

Materials and Methods

Materials

Stainless steel disks (SUS 316L; diameter: 12 mm or 25 mm; composition (% by atoms): C < 0.08, Si < 1.00, Mn < 2.00, P < 0.045, S < 0.030, Ni = 10.00~14.00, Cr = 16.00~18.00, Mo = 2.00 ~ 3.00, Fe = balance; Tsubame Bussan Co. Ltd., Niigata, Japan) were used as a model material for orthodontic dental brackets. Ultrapure Milli-Q water was used throughout this study. Diethanolamine (DEA), isopropanol (*i*-PrOH), and titanium isopropoxide (TTIP) (Nacalai Tesque, Inc., Kyoto, Japan) were used as reagents in the precursor solution. Acetone and nitric acid (Wako Pure Chemical Industries, Ltd., Osaka, Japan) were used for organic compound removal. Anatase (average particle size of 24 nm) and rutile particles (average particle size of 410 nm) (Sigma-Aldrich Corporation, St. Louis, MO, USA) were used to modify the precursor solution.

TiO_2 coating

The precursor solution for the TiO_2 coating was prepared by the following method [11]. First, DEA was dissolved in *i*-PrOH, and TTIP (0.1 mol/L) was subsequently added to the solution at room temperature. After the solution was stirred at 300 rpm for 2 h at room temperature, a water/isopropanol (1/10 in volume ratio) solution was added drop-wise under vigorous stirring to prepare a clear precursor solution for the TiO_2 coating. The final molar ratio of the solution containing TTIP/DEA/water was 1/1/1.

In order to prepare the modified precursor solution, commercially available anatase or rutile particles were added to the precursor solution (TiO_2 formed from TTIP / TiO_2 of the particles added (w/w) = 7/3). The solution was subjected to sonication for 5 min to disperse the particles which had been added to it. The uncoated stainless steel substrates were cleaned by acetone and concentrated nitric acid, washed with water, and then dried at room temperature. The TiO_2 coating was produced by dropping 74 μL of the above solution onto the stainless steel substrate, drying at room temperature, treating thermally at 600 °C (heating rate: 10 °C/min) for 30 min in air on a crucible in a horizontal furnace, and then cooling naturally in the furnace to room temperature. Coatings with different thicknesses were prepared by repeating the above procedure three or five times.

Characterization

The crystal phase of TiO_2 formed on the substrate was identified with an X-ray diffraction (XRD) apparatus (XRD-6100; Shimazu Corp., Kyoto Japan) equipped with a Cu-Kα radiation source. The weight ratio of anatase and rutile was determined from the intensity ratio of the 2θ peaks at 25.3 (anatase) and 27.5° (rutile), and a calibration curve was prepared from XRD measurements of a mixture of commercially

available anatase and rutile particles. X-ray photoelectron spectroscopy (XPS) measurements were conducted to determine the elemental distributions by depth using a PHI X-tool (Ulvac-Phi, Inc., Kanagawa, Japan) equipped with an Al-Kα radiation source (15 kV; 48 W; Acquisition Area: 204 nm) at a pass energy of 140.00 eV, a step size of 0.250 eV, Ar sputtering of 5 kV (approximately 368 nm/sweep), sweeps of 40, and a takeoff angle of 45° for Ti2p, O1s, Fe2p3, Ni2p3, Cr2p3, and C1s. The thickness of the coating layer was determined based on the point at which the Ti concentration started to decrease in the depth profile. The surface composition of Fe, Ni, and Cr were compared at the depth of 0 nm (*i.e.*, no Ar sputtering). The measurements were conducted for three randomly selected points on each sample, and the data were presented as means ± standard deviations of the mean (N=3). The surface microstructure of the coating was observed by scanning electron microscopy (SEM) using a 5 kV S-4800 (Hitachi High Technologies Corp., Tokyo, Japan) after the sample was sputter coated with Pt-Pd.

Photocatalytic activity

The photocatalytic activity of the TiO_2 coating was evaluated from the degradation rate of a methylene blue solution as follows. A silicon tube (inner diameter: 12 or 25 mm depending on the size of sample; height: approximately 1 cm) was fitted on the circumference of the sample disks, and 2 mL of the methylene blue solution (0.02 mmol/L) was poured into the silicone tube. The sample was placed approximately 1 cm away from a UV lamp (TOP® UV IRRADIATOR; wavelength, 300-400 nm with a peak centered at 352 nm) and irradiated for 1 h. A portion of the methylene blue solution (100 μL) was removed every 15 min, and the absorbance was measured using a SpectraMax M5 (Molecular Devices, Sunnyvale, CA, USA) at a wavelength of 664 nm.

Bacterial adhesion

The amount of adhered bacteria on the substrate was evaluated by the following method. The *Actinomyces oris* strain MG-1, which is one of the primary bacteria that initiates the formation of biofilms on teeth [34, 35], was grown aerobically in a heart infusion broth (HIB, Difco Laboratories) at 37 °C overnight. The TiO_2 coated substrates (no particle addition, anatase particle addition and rutile particle addition) were used after cleaning and sterilizing with an autoclave. Four milliliters of culture were inoculated into 36 mL of heart infusion broth (HIB) supplemented with 0.2% sucrose. The TiO_2 coated substrates were placed in each hole of a 24-well plate and incubated with bacteria at 37 °C under aerobic conditions. After 16 h, the culture supernatant was removed from the 24-well plate and the substrates were washed with distilled water. The substrates were then stained with 0.5% crystal violet for 10 minutes and washed with distilled water. The substrates were carefully transferred to another 24-well plate and then dipped in 1 mL of 95% ethanol for 1 h. The absorbance of the extracted crystal violet was measured at 590 nm using a Spectra Max M5. Uncoated stainless steel substrates were used as a control.

Results

Gloss observation

Figure 1 shows digital photographs of the surface of TiO_2 coated three times on SUS 316L stainless steel substrates. In the case of the conventional sol-gel method without particle addition (Fig. 1a), the coating layer was transparent and the stainless steel substrate could be observed through the coating layer. In contrast, opaque coating layers were obtained and the metal color was shielded when the modified sol-gel methods incorporating both kinds of particle addition were used (Figs. 1b and c).

SEM observation

Figure 2 shows SEM images of the surface of the TiO_2 coatings. In the case of the conventional sol-gel method (Fig. 2a), dense coating layers were formed and cracks were not observed regardless of the number of coatings. For the modified sol-gel methods with both types of particle addition, microcracks were observed for single coatings (Figs. 2b-1, c-1) and the cracks were filled by repeated coatings (Figs. 2b-2 and 2b-3 for anatase particle addition; 2c-2 and 2c-3 for rutile particle addition).

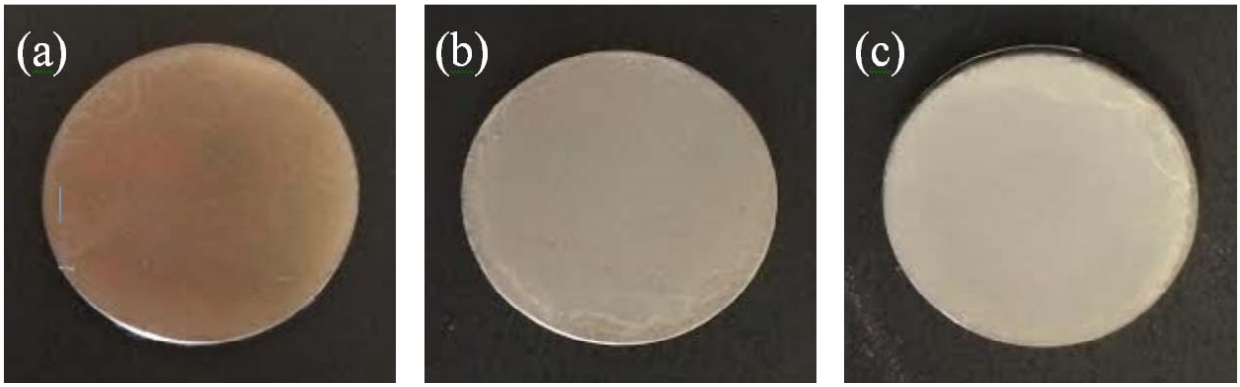

Fig. 1 The surface color of three TiO_2 coatings on stainless substrates: (a) no particle addition; (b) anatase particle addition 7/3; (c) rutile particle addition 7/3

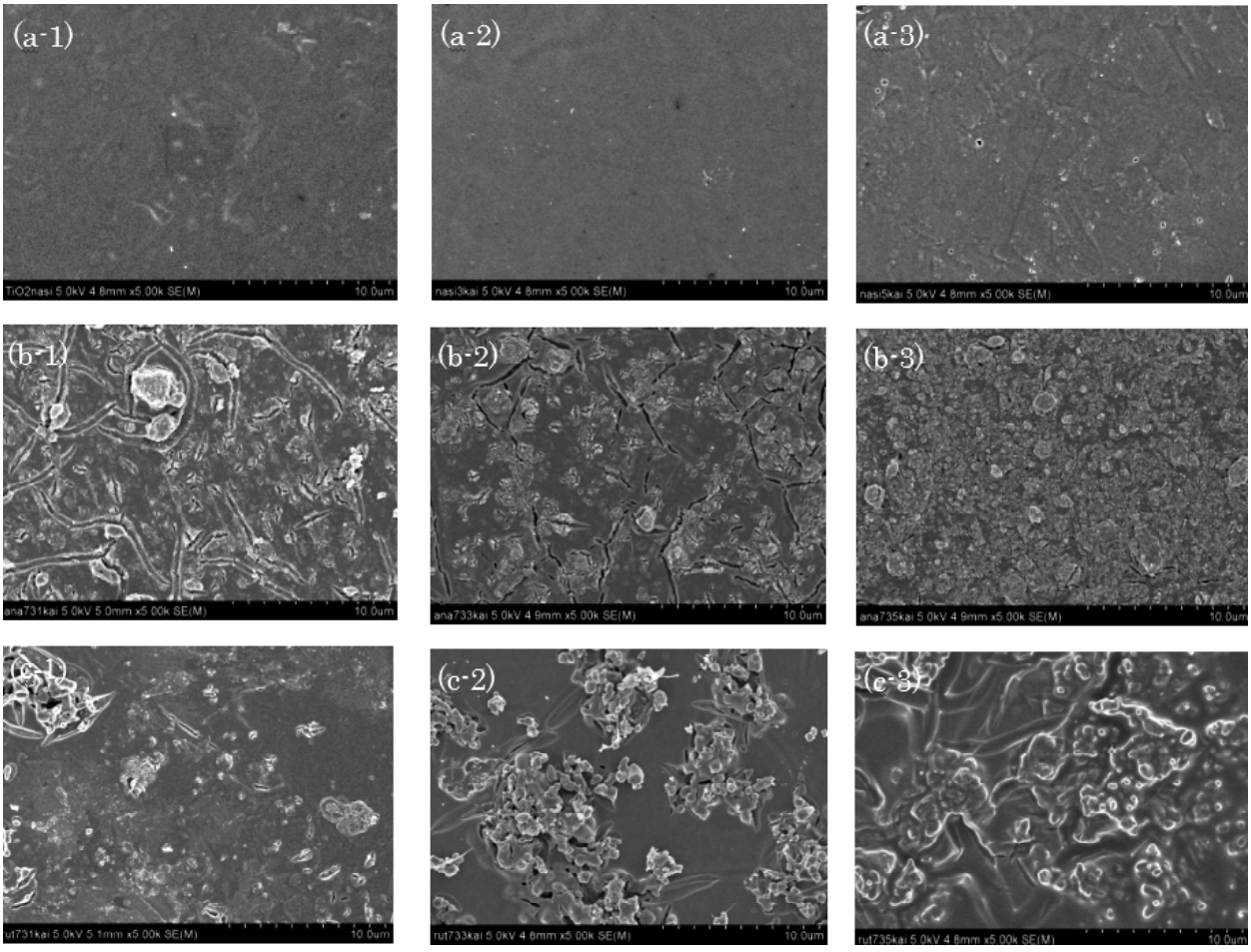

Fig. 2 SEM surface images of the TiO_2 coatings on stainless substrates: (a) no particle addition; (b) anatase particle addition 7/3; (c) rutile particle addition 7/3; 1: single coating; 2: three coatings; 3: five TiO_2 coatings

XRD analysis

Figure 3 shows the XRD patterns of the TiO_2 coated substrates. The intensities of the diffraction peak at 25.3° (anatase) increased with the increase in the number of coatings for all types of sol-gel coatings. In the case of the conventional coating (Fig. 3a) and the modified coating with anatase particles, a rutile phase could not be detected. On the other hand, in the case of the modified coating with rutile particles, a binary crystalline phase consisting of anatase and rutile was observed on the substrate (Fig. 3c). The anatase/rutile weight ratios varied from the theoretical value (7/3) calculated from the loading ratio of TTIP and rutile TiO_2 particles under the assumption that the TiO_2 formed from TTIP was anatase, and the determined anatase/rutile weight ratios were as follows: 4.6/5.4 for a single coating; 4.9/5.1 for three coatings (c-2); and 6.3/3.7 for five coatings.

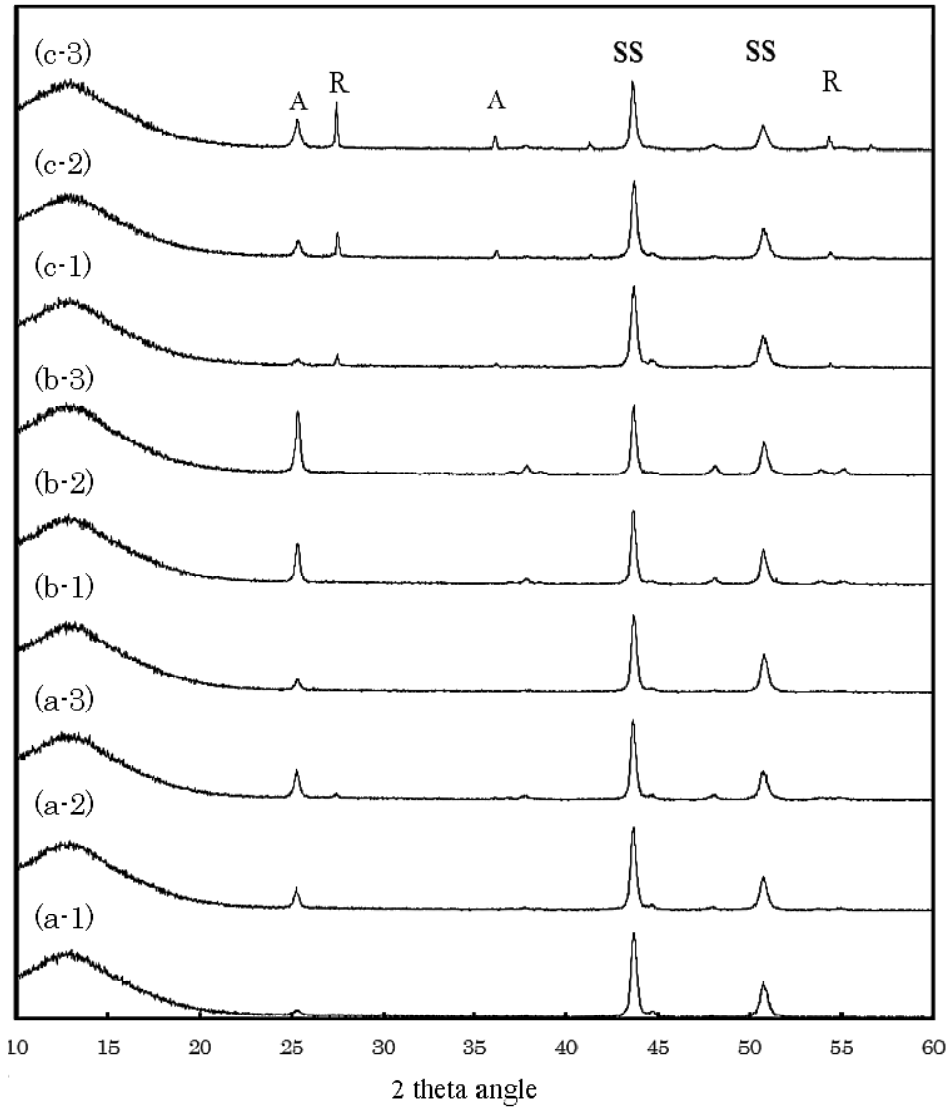

Fig. 3 XRD patterns of the TiO_2 coatings on stainless steel substrates at different numbers of coatings: (a) no particle addition; (b) anatase particle addition 7/3; (c) rutile particle addition 7/3; 1: single coating; 2: three coatings; 3: five TiO_2 coatings

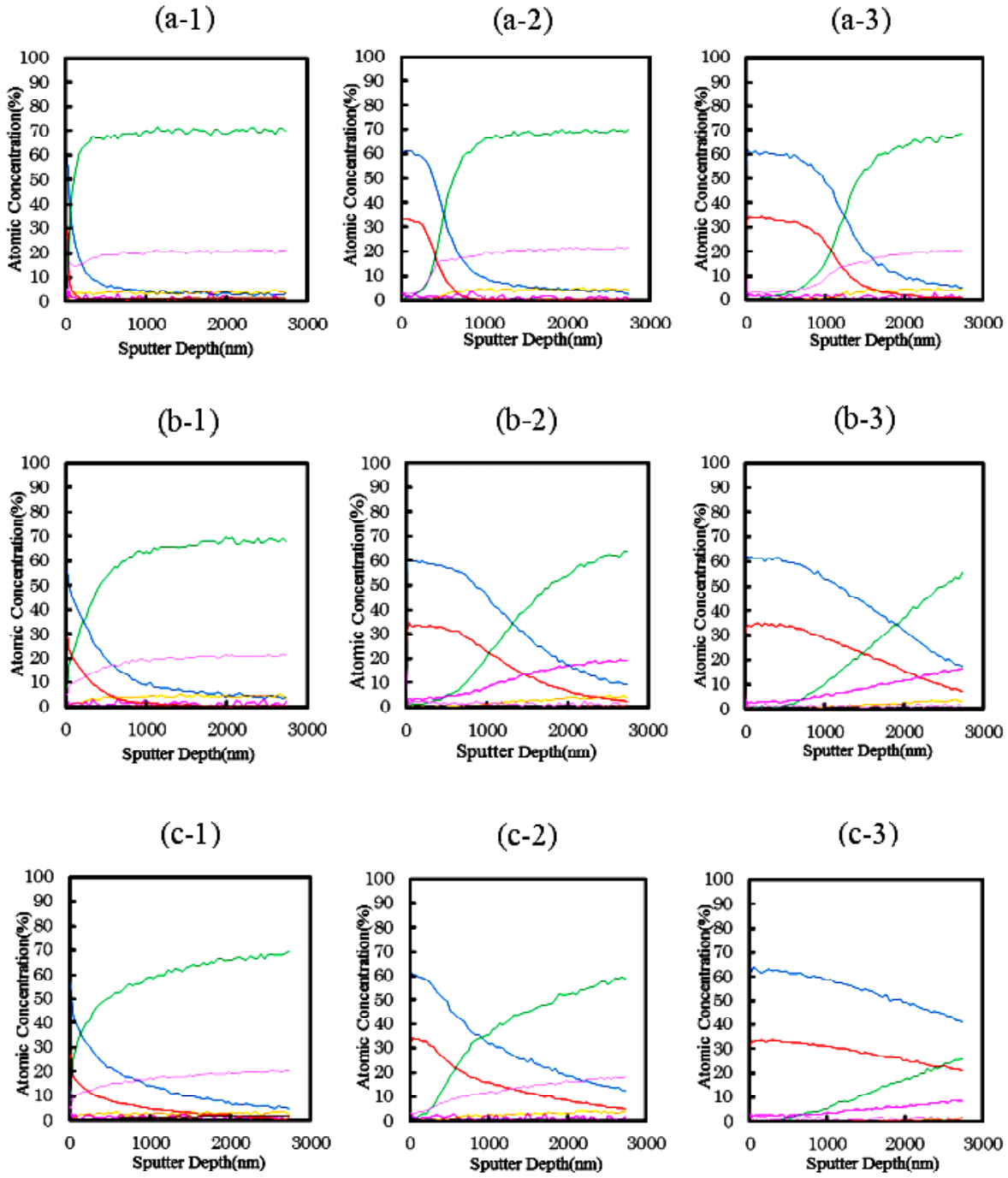

Fig. 4 XPS(depth) of the TiO_2 coatings on stainless substrates: (a) no particle addition; (b) anatase particle addition 7/3; (c) rutile particle addition 7/3; 1: single coating; 2: three coatings; 3: five TiO_2 coatings

XPS analysis

The elemental depth profiles (Ti, O, Fe, Ni, Cr and C; see Fig. 4), the thicknesses (Fig. 5), and surface compositions (Fig. 6) of the TiO_2 coatings were compared. The thickness of the TiO_2 coating layer in each case increased with an increase in the number of coatings. Both Fe and Cr included in the stainless steel substrates were detected, but Ni was not detected. The ratio of Fe decreased while the ratio of Cr did not change with an increasing number of coatings.

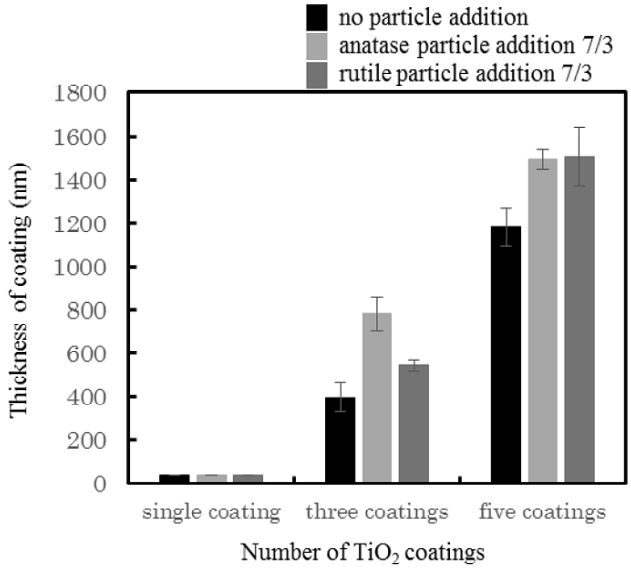

Fig. 5 Film thickness of the TiO_2 films at different numbers of TiO_2 coatings.

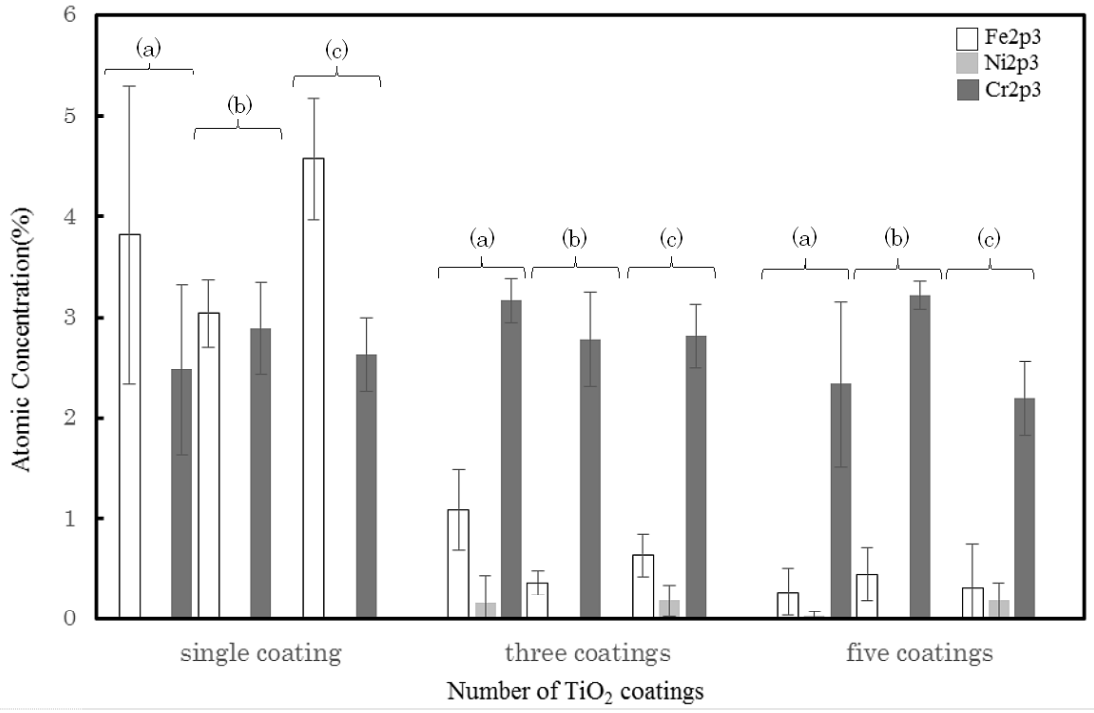

Fig. 6 XPS(depth) of the composition of TiO_2 coatings layers: (a) no particle addition; (b) anatase particle addition 7/3; (c) rutile particle addition 7/3

Photocatalytic activity

Figure 7 shows the photocatalytic activities of the TiO_2 coated stainless steel substrates determined from the degradation rate of methylene blue. The rutile particle addition (TiO_2 formed from TTIP/ TiO_2 of the particles added (w/w) = 7/3) (Fig. 7c) with three coatings had the quickest degradation speed of 0.02 mmol/L methylene blue solution. The anatase particle addition (TiO_2 formed from TTIP/ TiO_2 of the particles

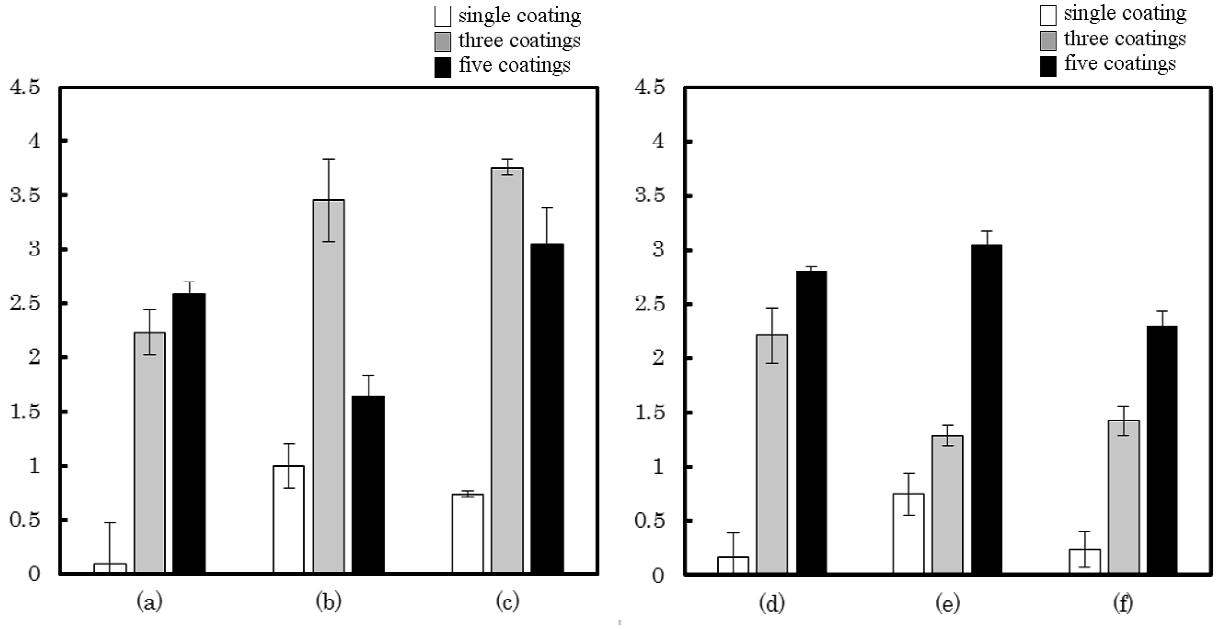

Fig. 7 Photocatalytic performance of specimens evaluated using the degradation speed of methylene blue solution: (a) no particle; (b) anatase 7/3; (c) rutile 7/3; (d) rutile 9.5/0.5; (e) rutile 9/1;(f) rutile 8/2

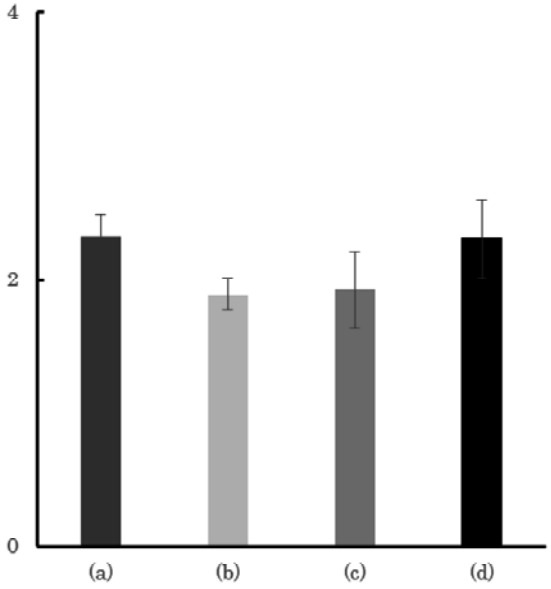

Fig. 8 Amount of adhered oral *Actinomyces* on the substrate (no UV irradiation) (a) no particle addition; (b) anatase particle addition 7/3, single coating; (c) rutile particle addition 7/3, single coating; (d) control.

added (w/w) =7/3) (Fig. 7b) with three coatings was the second quickest. An apparent correlation between increasing degradation rates and number of coatings was observed for coatings with no particle addition (Fig. 7a), as well as with rutile particle addition at ratios of 9.5/0.5 (Fig. 7d), 9/1 (Fig. 7e) and 8/2 (Fig. 7f). No apparent correlation between degradation rates and number of coatings was observed for either anatase (Fig. 7b) or rutile (Fig. 7c) additions at a ratio of 7/3.

Bacterial adhesion

Figure 8 shows the amount of adhered *Actinomyces oris* MG-1 on the samples. While slight differences between the substrate with the TiO_2 coating and the control samples were observed under the dark conditions conducted in this study, the results were not considered to be significant.

Discussion

Stainless steels have been frequently used in orthodontic dental brackets due to their mechanical properties and low cost. There is, however, concern regarding the effects of the high-temperature treatment, e.g., decreased mechanical properties due to the microstructural changes induced by the heat treatment of high-carbon content stainless steel at 650 °C [36]. Therefore, the development of a TiO_2 sol-gel coating at low temperature is needed, though binary TiO_2 crystal phases are generally obtained at treatment temperatures > 600 °C [37]. In this study, a binary TiO_2 crystal phase was prepared by the modified sol-gel method using as-prepared rutile particles.

Titanium dioxide particles have been industrially used as a white pigment for papers and paints due to their high refractive index (*i.e.*, light scattering efficiency). The TiO_2 coating layer formed by the conventional sol-gel method without particle addition was transparent, whereas the layer formed by the modified methods effectively shielded the metallic color of the stainless steel substrate, which was attributed to the light scattering efficiency of the added particles. The opaque coating should be useful for improving the aesthetics of orthodontic dental brackets.

In the SEM observation, the surface roughness of the coating layer increased in the case of the modified method that incorporated rutile particles, compared to the conventional method. This was thought to be because the particle size was relatively large (410 nm) and some particles likely aggregated during the coating procedure. The surface roughness problem could be solved by using smaller sized rutile particles with higher dispersibility in the liquid media.

A TiO_2 coating layer with a binary crystal phase was obtained *via* a low temperature treatment (600 °C) by adding rutile particles to the precursor solution. The composition (anatase/rutile ratio) of the TiO_2 coating layer was easily controlled by changing the amount of rutile particles added. Note that the rutile/anatase ratio tended to be larger than the ratio calculated from the amount of rutile particles added, which might have been due to the rutile particles acting as an epitaxial nucleation/growth site for TiO_2 crystals formed from TTIP decomposition. Ghasemi *et al* [38], reported that transition metal (Fe, Cr, Mn, Co, Ni, Cu and Zn) doped TiO_2 nanoparticles exhibit higher photocatalytic activity than pure TiO_2, and that Fe and Cr can catalyze anatase–rutile transformation. Therefore, the migration of Fe and Cr ions from stainless steel substrates into the coating layer might also assist with the transition of anatase to rutile in the presence of rutile particles.

The TiO_2 coating layer of a single crystal phase (*i.e.*, anatase) was also obtained in the case of the modified method with anatase particles, suggesting that the composition of the TiO_2 coating layer could also be easily controlled by changing the mix ratio of rutile/anatase particles. When comparing the number of coatings, the photocatalytic activity improved with an increased number of coatings for all coatings in each training ratio (Fig. 7a, d-f), though this trend was not observed for anatase 7/3 (Fig. 7b) and rutile 7/3 (Fig. 7c). The reason for the improvement in photocatalytic activity with an increased number of coatings was attributed to the increased thickness of the TiO_2 coating layer, which would absorb more light with an increased number of coatings. The largest photocatalytic activity measured in this study was from the TiO_2 coating prepared using the rutile particles (TiO_2 formed from TTIP/TiO_2 of parti-

cle (w/w) =7/3) with three coatings. These results suggest that the composition of transition metal (especially, Fe), which decreased with an increased number of coatings (*i.e.*, coating thickness), is also important to improve the photocatalytic activity.

In the result of bacteria adhesion examination, a significant difference was not obtained between the TiO_2 coating and control sample. This result suggested that the degree of bacteria adhesion did not change between the TiO_2 coating and control when there was no UV irradiation.

Conclusion

In this study, we investigated the structure of TiO_2 coating layers on stainless steel substrates that are frequently used as the main material in orthodontic dental brackets. We also compared the photocatalytic activity of TiO_2 coatings with no particles to coatings with anatase or rutile particles added. We demonstrated that Fe and Cr concentrations in the TiO_2 coatings layer were the largest in a single coating with rutile particle addition. We also demonstrated that increasing the total number of coatings resulted in higher photocatalytic activity compared to single coatings. The TiO_2 coating with a controllable binary crystal phase can potentially contribute to the development of photocatalytic orthodontic dental brackets for improving oral health during orthodontic treatments.

References

1) Albert G, Jackson B, Thomas W. Orthodontic dental patients and expenditures-2004. Am J Orthod Dentofacial Orthop 2008; 134: 337–343.
2) Kubo Y, Horiuchi K, Furuta H, Nomura D, Kobuchi M, Mushimoto K. Clinico-statistical observation of orthognathic surgery in the first department of oral and maxillofacial surgery, Osaka dental university hospital, concerning the past 20 years. Jpn J Jaw Deform 2003; 13: 44–51. (Japanese)
3) Matsumoto M, Nakashima S, Itoh T, Hirose T, Kawai S, Yanabu M, Kiyosue T, Kido K, Inudou K, Tominaga M, Oniki Y, Shimoda T, Gondo S, Arakawa N, Sakamoto M, Okina H, Hong S, Matsuo T, Kunitake H, Tanaka K, Aoki K and Fujie T. Statistical investigation on orthodontic patients who received treatment at Fukuoka dental college during the past 20 years. J Fukuoka Dent Coll 1995; 22: 143–152. (Japanese)
4) Isono A, Shimada T, Amano K and Kuwahara Y. Caries risk evaluation in orthodontic patients treated with multi-bracket appliances. Tsurumi Shigaku 2001; 27: 261–272. (Japanese)
5) Boersma JG, Veen MH, Lagerweij MD, Bokhout B, Prahl-Anderson B. Caries prevalence measured with QLF after treatment with fixed orthodontic appliances: influencing factors. Caries Res 2005; 39: 41–47.
6) Ögaard B. Prevalence of white spot lesions in 19-year-olds: a study on untreated and orthodontically treated persons 5 years after treatment. Am J Orthod Dentofacial Orthop 1989; 96: 423–427.
7) Mattingly JA, Sauer GJ, Yancey JM and Arnold RR. Enhancement of streptococcus mutans colonization by direct bonded orthodontic appliances. J Dent Res 1983; 62: 1209–1211.
8) Ewa M, Czochrowska, Marco R. The orthodontic/periodontal interface. Semin Orthod 2015; 21: 3–14.
9) Robert ML, Richard AR and Jon A. An evaluation of changes in mandibular anterior alignment from 10 to 20 years postretention. Am J Orthod Dentofacial Orthop 1988; 93: 423–428.
10) William SP. Retention-retainers may be forever. Am J Orthod Dentofacial Orthop 1989; 95: 505–513.
11) Takahashi Y, Matsuoka Y. Dip-coating of TiO2 films using a sol derived from Ti(O-i-Pr) 4-diethanolamine-H2O-i-PrOH system. J Mater Sci 1988; 23: 2259–2266.
12) Yu JC, Ho W, Lin J, Yip H and Wong PK. Photocatalytic activity, antibacterial effect, and photoinduced hydrophilicity of TiO_2 films coated on a stainless steel substrate. Environ Sci Technol 2003; 37: 2296–2301.
13) Chen Y, Dionysiou DD. Effect of calcination temperature on the photocatalytic activity and adhesion of TiO^2 films prepared by the P-25 powder-modified sol-gel method. J Mol Catal A Chem 2006; 244: 73–82.
14) Koseki H, Shiraishi K, Asahara T, Tsurumoto T, Shindo H, Baba K, Taoda H and Terasaki N. Photocatalytic bactericidal action of fluorescent light in a titanium dioxide particle mixture: an in vitro study. Biomed Res 2009; 30: 189–192.
15) Sato Y, Miyazawa K, Sato N, Nakano K, Takei Y, Kawai T and Goto S. Study on fabrication of orthodontic brackets with the photocatalytic function of titanium dioxide. Dent Mater J 2009; 28: 388–395.
16) Chen X, Wang X and Fu X. Hierarchical macro/mesoporous TiO_2/SiO_2 and TiO_2/ZrO_2 nanocomposites for environmental photocata-

lysis for environmental photocatalysis. Energy Environ Sci 2009; 2: 872–877.
17) Kiser MA, Westerhoff P, Benn T, Pérez-Rivera J and Hristovski K. Titanium nanomaterial removal and release from wastewater treatment plants. Environ Sci Technol 2009; 43: 6757–6763.
18) Kishi A, Otsuki M, Sadr A, Ikeda M and Tagami J. Effet of light units on tooth bleaching with visible-light activating titanium dioxide photocatalyst. Dent Mater J 2011; 30: 723–729.
19) Saita M, Kobatashi K, Yoshino F, Hase H, Nonami T, Kimoto K and Lee MC. ESR inbestigation of ROS generated by H_2O_2 bleaching with TiO_2 coated Hap. Dent Mater J 2012; 31: 458–464.
20) Lu L, Yoshikawa K, Komatsu O, Hirota Y, Hattori Y, Inoue C, Yasuo K, Tanimoto H, Iwata N, Wu B and Yamamoto K. Evaluation of a tooth bleaching system incorporating titanium dioxide. J Osaka Dent Univ 2013; 47: 209–214.
21) Jie Z, Nosaka Y. Mechanism of the OH radical generation in photocatalysis with TiO_2 of different crystalline types. J Phys Chem C 2014; 118: 10824–10832.
22) Sclafani A, Herrmann JM. Comparison of the photoelectronic and photocatalytic activities of various anatase and rutile forms titania in pure liquid organic phases and in aqueous solutions. J Phys Chem 1996; 100: 13655–13661.
23) Kawahara T, Ozawa T, Iwasaki M, Tada H and Ito S. Photocatalysic activity of rutile-anatase coupled TiO_2 particles prepared by a dissolution-reprecipitation method. J Colloid Interface Sci 2003; 267: 377–381.
24) Ohno T, Tokieda K, Higashida S and Matsumura M. Synergism between rutile and anatase TiO2 particles in photocatalytic oxidation of naphthalene. Appl Catal A Gen 2003; 244: 383–391.
25) Bakardjieva S, Šubrt J, Štengl V, Dianez MJ and Savagues MJ. Photoactivity of anatase-rutile TiO_2 nanocrystalline mixtures obtained by heat treatment of homogeneously precipitated anatase. Appl Catal B 2005; 58: 193–202.
26) Bojinova A, Kralchevska R, Poulios I and Dushkin C. Anatase/rutile TiO_2 composites: Influence of the mixing ratio on the photocatalytic degradation of Malachite Green and Orange II in slurry. Mater Chem Phys 2007; 106: 187–192.
27) Meulen T, Mattson A and Österlund L. A comparative study of the photocatalytic oxidation of propane on anatase, rutile, and mixed-phase anatase-rutile TiO_2 nanoparticles: Role of surface intermediates. J Catal 2007; 251: 131–144.
28) Tomaszewski H, Poelman H, Depla D, Heynderickx G and Marin GB. TiO_2 films prepared by DC magnetron sputtering from ceramic targets. Vacuum 2002; 68: 31–38.
29) Yang TS, Shiu CB and Wong MS. Structure and hydrophilicity of titanium oxide films prepared by electron beam evaporation. Surf Sci 2004; 548: 75–82.
30) Borrero-López O, Hoffman M, Bendavid A and Martin PJ. Mechanical properties and scratch resistance of filtered-arc-deposited titanium oxide thin films on glass. Thin Solid Films 2011; 519: 7925–7931.
31) Fu T, Wen CS, Lu J, Zhou YM, Ma SG, Dong BH and Liu BG. Sol-gel derived TiO_2 coating on plasma nitrided 316L stainless steel. Vacuum 2012; 86: 1402–1407.
32) Chiu KY, Wong MH, Cheng FT and Man HC. Characterization and corrosion studies of titania-coated NiTi prepared by sol-gel technique and steam crystallization. Appl Surf Sci 2007; 253: 6762–6768.
33) Oh KT, Kim YS, Park YS and Kim KN. Properties of super stainless steels for orthodontic applications. J Biomed Mater Res B Appl Biomater 2004; 69: 183–194.
34) Omae A, Yamane K and Matsumoto N. Biofilm formation of Actinomyces oris strain MG-1 on an orthodontic wire. J Osaka Dent Univ 2013; 47: 75–82.
35) Yeung MK. Molecular and genetic analyses of Actinomyces spp. Crit Rev Oral Biol Med 1999; 10: 120–138.
36) Weiss B, Stickler R. Phase instabilities during high temperature exposure of 316 austenitic stainless steel. Metal Trans 1972; 3: 851–866.
37) Hanaor DAH, Sorrell CC. Review of the anatase to rutile phase transformation. J Mater Sci 2011; 46: 855–874.
38) Ghasemi S, Rahimnejad S, Rahman Setayesh S, Rohani S and Gholami MR. Transition metal ions effect on the properties and photocatalytic activity of nanocrystalline TiO_2 prepared in an ionic liquid. J Hazard Mater 2009; 172: 1573–1578.

(Received: October 23, 2015/
Accepted: December 19, 2015)

Corresponding authors:
Mayuko Awata, D.D.S
[1]Graduate School of Dentistry
(Department of Orthodontics),
Osaka Dental University
8-1 Kuzuhahanazono-cho, Hirakata-shi,
Osaka 573-1121, Japan
Tel: +81-72-864-3078
Fax: +81-72-864-3178
E-mail: awamayu0219@gmail.com

Masahiro Okada, Ph.,D.
Department of Biomaterials,
Graduate School of Medicine,
Dentistry and Pharmaceutical Sciences,
Okayama University
2-5-1 Shikada-cho, Kita-ku, Okayama-shi,
Okayama 700-8558, Japan
Tel&Fax: +81-86-235-6666
E-mail: m-okada@cc.okayama-u.ac.jp